Chemical diffusivity of $BaTiO_{3-\delta}$: Defect chemical analysis

Chang-Rock Song and Han-Ill Yoo*

Solid State Ionics Research Laboratory, School of Materials Science and Engineering, Seoul National University, Seoul 151-742, Korea

(Received 11 January 1999; revised manuscript received 24 August 1999)

The chemical diffusivity of undoped $BaTiO_{3-\delta}$ which was measured in Song and Yoo [Solid St. Ionics **120**, 141 (1999)] is analyzed on the basis of the defect structure proposed and Wagner's classic theory of chemical diffusion. It is confirmed that a maximum of isothermal chemical diffusivity around the stoichiometric composition ($\delta=0$) is of thermodynamic origin. The combination of the isotherms of both electrical conductivity and chemical diffusivity enables one to evaluate, without recourse to any assumption at all, the concentration product of electrons and holes, $K_i(=np)$, as well as the mobilities of electrons and holes, μ_n and μ_p, separately.

I. INTRODUCTION

In a previous paper,[1] we have determined by a conductivity relaxation technique the chemical diffusion coefficient ($\tilde{D}$) of "undoped" [meaning not intentionally doped but containing background (acceptor) impurities]. $BaTiO_{3-\delta}$ against oxygen partial pressure (P_{O_2}), in the widest ever range of $10^{-16} \leqslant P_{O_2}/atm \leqslant 1$ at elevated temperatures of 800, 900, 1000, and 1100 °C, respectively. The result, $\tilde{D}$ vs $\log_{10} P_{O_2}$, is as shown in Fig. 1. The equilibrium, total conductivity (σ) of the same specimens is also shown in Fig. 2. Upon comparison, it is seen that, over the n-to-p transition region of P_{O_2} across the conductivity minimum on a conductivity isotherm, the corresponding chemical diffusivity varies convex upwardly with $\log_{10} P_{O_2}$, leaving a maximum approximately at the oxygen partial pressure where the conductivity minimum falls. This sort of behavior of $\tilde{D}$ has never been observed in oxide systems.

In this paper, we will analyze the chemical diffusivity of Fig. 1 in the light of Wagner's classic theory of chemical diffusion[2] and the defect structure[3] of $BaTiO_3$ proposed. The present analysis consequently enables one to evaluate the concentration product of electrons and holes (i.e., $np=K_i$) and the mobilities of electrons and holes (μ_n, μ_p) separately, without having recourse to any assumption at all. We will begin by briefly reviewing the defect structure and transport properties of the system.

II. DEFECT STRUCTURE AND TRANSPORT PROPERTIES OF UNDOPED $BaTiO_3$

A. Defect structure

The irregular structure elements in undoped $BaTiO_3$ may be electrons (e'), holes ($h^{\cdot}$), oxygen vacancies ($V_O^{\cdot\cdot}$), cation vacancies (V_{Ba}'' and V_{Ti}''''), and acceptor-type background impurities (A_C'), as the possibility of interstitial disorders are ruled out from a structural viewpoint.[3-5] In order to calculate the equilibrium concentrations of these defects as functions of the thermodynamic variables of the system, temperature (T), the activity of oxygen ($a_{O_2} \equiv P_{O_2}/atm$), and the activity

of a metallic component, say, BaO (a_{BaO}), at atmospheric pressure, one may consider the two external equilibria:

$$O_o^\times = V_O^{\cdot\cdot} + 2e' + \frac{1}{2}O_2(g); \quad K_R = [V_O^{\cdot\cdot}]n^2 P_{O_2}^{1/2}, \quad (1)$$

$$BaO = Ba_{Ba}^\times + O_o^\times + V_{Ti}'''' + 2V_O^{\cdot\cdot}; \quad K_B = \frac{[V_{Ti}''''][V_O^{\cdot\cdot}]^2}{a_{BaO}} \quad (2)$$

and the two internal equilibria:

$$0 = e' + h^{\cdot}; \quad K_i = np, \quad (3)$$

$$0 = V_{Ba}'' + V_{Ti}'''' + 3V_O^{\cdot\cdot}; \quad K_s = [V_{Ba}''][V_{Ti}''''][V_O^{\cdot\cdot}]^3, \quad (4)$$

along with the charge neutrality condition:

$$n + 2[V_{Ba}''] + 4[V_{Ti}''''] + [A_c'] = p + 2[V_O^{\cdot\cdot}], \quad (5)$$
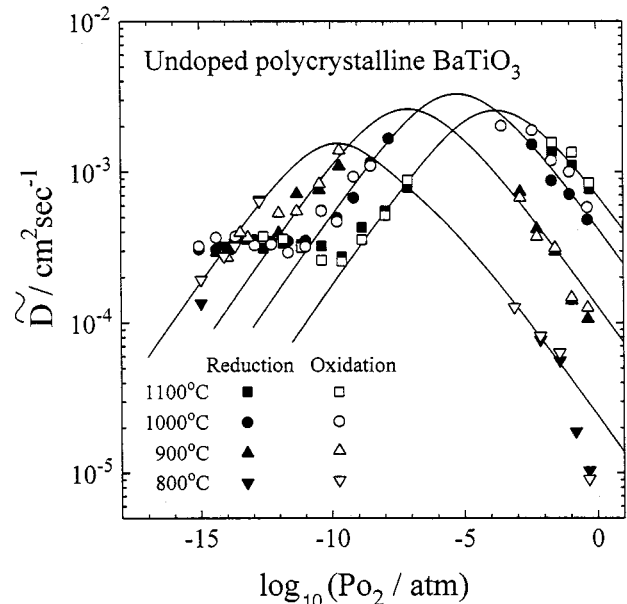
FIG. 1. Chemical diffusivity of undoped $BaTiO_3$ against oxygen partial pressure at different temperatures. The solid lines are the best fitted to Eq. (24) in the text.
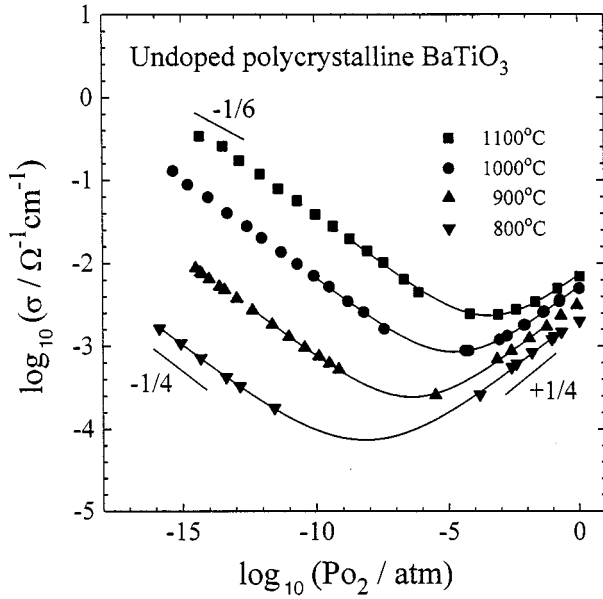
FIG. 2. Total electrical conductivity of undoped $BaTiO_3$ against oxygen partial pressure at different temperatures (Ref. 1). The solid lines are the best fitted to Eq. (18) in the text.

FIG. 3. Configuration of the majority disorder types depending on the thermodynamic variables $\log_{10} P_{O_2}$ and a_{BaO} at a given temperature when $[A_C'] \gg K_s^{1/2}, K_i^{1/2}$, where m denotes the oxygen partial pressure exponent of electronic carrier densities such that $p \propto P_{O_2}^m$ and $n \propto P_{O_2}^{-m} (m \geq 0)$.[3] A dotted line presents a possible path as observed experimentally along which the activity of a metallic component is kept constant.

where [ ] denote the concentration of the irregular structure elements therein ($n \equiv [e']$ and $p \equiv [h^\cdot]$). The mass-action law constant of the relevant reaction is denoted as $K_j (j = R, B, S, i)$, which may be represented as

$$K_j = K_j^0 \exp\left(-\frac{\Delta H_j}{kT}\right),\qquad(6)$$

where K_j^0 is a preexponential factor and ΔH_j the enthalpy change of the relevant reaction j.

At a given temperature, seven majority disorder regimes can thus be distinguished depending on a_{BaO} and P_{O_2} as shown in Fig. 3.[3] It is noted that when $[A_C'] \rightarrow 0$, the regimes $(h^\cdot, A_C')$ and $(A_C', V_O^{\cdot\cdot})$ shrink to a point and a vertical line, respectively, rendering the regimes $(V_O^{\cdot\cdot}, V_{Ba}'')$ and $(V_O^{\cdot\cdot}, V_{Ti}'''')$ to directly neighbor with each other. In the intermediate range of P_{O_2} (between the n-type and p-type regimes), one finds the three ionic disorder regimes $[V_{Ba}''] \approx [V_O^{\cdot\cdot}]$, $[A_C'] \approx 2[V_O^{\cdot\cdot}]$, and $2[V_{Ti}''''] \approx [V_O^{\cdot\cdot}]$ in turn as a_{BaO} increases. In all these regimes, the oxygen vacancy concentration is essentially fixed and the concentrations of electrons and holes vary with P_{O_2} as $n \propto P_{O_2}^{-1/4}$ and $p \propto P_{O_2}^{+1/4}$ as can be shown by solving Eqs. (1)–(4) in association with each of these limiting neutrality conditions.[3] It, however, has never been unambiguously determined which type is really predominant in the P_{O_2} region where the electronic conductivity varies as $\sigma_{el} \propto P_{O_2}^{\pm 1/4}$.[3,4] Furthermore, none of the exclusively p-type regimes, $(h^\cdot, A_C')$, $(h^\cdot, V_{Ba}'')$, and $(h^\cdot, V_{Ti}'''')$ have ever been revealed themselves for the system of $BaTiO_3$ up to $P_{O_2} = 1$ atm. For simplicity, we thus introduce the effective concentration of monovalent acceptors, $[A'] (\equiv 2[V_{Ba}''] + 4[V_{Ti}''''] + [A_C'])$, to rewrite Eq. (5) as[1]

$$n + [A'] = p + 2[V_O^{\cdot\cdot}].\qquad(7)$$

One can, then, simplify, without loss of generality, the configuration of Fig. 3, neglecting the exclusively p-type regimes $(h^\cdot, A')$, only with two disorder regimes $(e', V_O^{\cdot\cdot})$ and $(A', V_O^{\cdot\cdot})$. The defect concentrations of present interest in each regime are calculated by using Eqs. (1), (3), (4), and (7) as follows:

(i) In the regime $(e', V_O^{\cdot\cdot})$,

$$[V_O^{\cdot\cdot}] = \frac{n}{2} = \left(\frac{K_R}{4}\right)^{1/3} P_{O_2}^{-1/6}.\qquad(8)$$

(ii) In the regime $(A', V_O^{\cdot\cdot})$,

$$[V_O^{\cdot\cdot}] = \frac{[A']}{2},\qquad(9)$$

$$n = \sqrt{K_i} \left(\frac{P_{O_2}}{P_{O_2}^0}\right)^{-1/4},\qquad(10)$$

$$p = \sqrt{K_i} \left(\frac{P_{O_2}}{P_{O_2}^0}\right)^{+1/4},\qquad(11)$$

where $P_{O_2}^0$ is such that $n = p = K_i^{1/2}$ or

$$P_{O_2}^0 = \left(\frac{2K_R}{[A']K_i}\right)^2.\qquad(12)$$

These defect concentrations are plotted against oxygen partial pressure, e.g., at 1000 °C in Fig. 4.
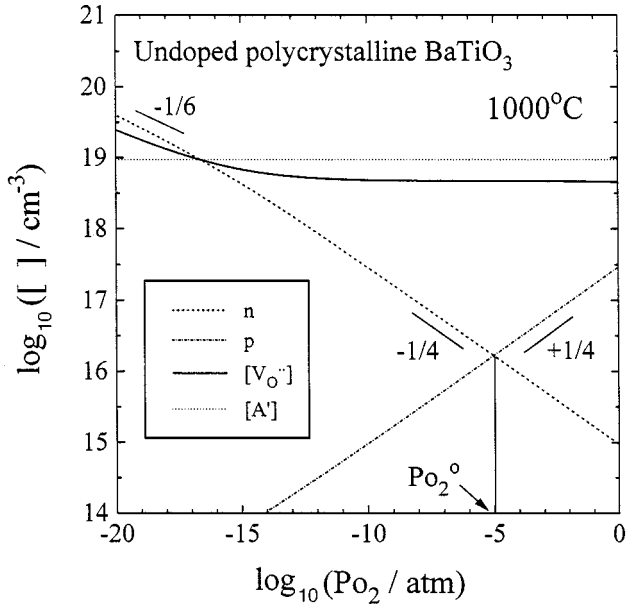
FIG. 4. Defect concentrations against oxygen partial pressure for undoped BaTiO$_3$ at 1000 °C. For the calculation the following values were used: $K_i/\text{cm}^{-6}=2.72\times10^{32}$, $K_R/\text{cm}^{-9}\text{ atm}^{1/2}=3.98\times10^{48}$, and $[A']/\text{cm}^{-3}=9.34\times10^{18}$ in accordance with the present analysis.

B. Electrical conductivity

It is reported that the self-diffusion coefficients of O and Ba are 4.58×10^{-12} and $5.28\times10^{-16}\text{ cm}^2\text{ sec}^{-1}$, respectively, e.g., at 1000 °C (the former in an atmosphere of $P_{O_2}=0.5$ atm and the latter presumably in air atmosphere),[6,7] and that the migration enthalpy of Ti ions is about 5 times larger than that of Ba ions.[5] We may thus assume that the cations, Ba^{2+} and Ti^{4+}, are practically immobile compared with the oxide ions at temperatures of present interest and regard only oxide anions O^{2-} (or, equivalently, $V_O^{\cdot\cdot}$) and electrons (or, equivalently, e' and $h^{\cdot}$) as the mobile, charged components (or, equivalently, structure elements). We may further assume that the mobilities of these charge carriers are independent of oxygen partial pressure. The total conductivity σ is then given in each of the defect regimes in Fig. 4 as follows:

(i) In the regime $(e', V_O^{\cdot\cdot})$, because $n\gg p$ and $\mu_n\gg\mu_{V_O}$ (where μ_n and μ_{V_O} are the mobility of e' and $V_O^{\cdot\cdot}$, respectively), the total conductivity in this regime is essentially the same as the conductivity of electrons (e'), σ_n, or, due to Eq. (8),

$$\sigma\approx\sigma_n=ne\mu_n=e\mu_n(2K_R)^{1/3}P_{O_2}^{-1/6}. \qquad (13)$$

(ii) In the regime $(A', V_O^{\cdot\cdot})$, the partial conductivities of electrons and holes, σ_n and σ_p, may be represented, due to Eqs. (10) and (11), as

$$\sigma_n=\frac{\sigma_{el,m}}{2}\left(\frac{P_{O_2}}{P_{O_2}^*}\right)^{-1/4}, \quad \sigma_p=\frac{\sigma_{el,m}}{2}\left(\frac{P_{O_2}}{P_{O_2}^*}\right)^{+1/4}, \quad (14)$$

where $\sigma_{el,m}$ is the minimum of the electronic total conductivity $\sigma_{el}(=\sigma_n+\sigma_p)$ and $P_{O_2}^*$ the corresponding oxygen partial pressure such that $\sigma_n=\sigma_p=\sigma_{el,m}/2$. These are given as[8,9]

$$\sigma_{el,m}=2e\sqrt{\mu_n\mu_p}\sqrt{K_i}, \qquad (15)$$

$$P_{O_2}^*=\left(\frac{2K_R}{[A']K_i}\right)^2\left(\frac{\mu_n}{\mu_p}\right)^2, \qquad (16)$$

respectively, where μ_p is the mobility of holes.

The ionic conductivity by oxygen vacancies, σ_{ion}, can be expressed due to the Nernst-Einstein equation as

$$\sigma_{ion}=\frac{4e^2[V_O^{\cdot\cdot}]D_{V_O}}{kT}, \qquad (17)$$

where D_{V_O} is the diffusivity of oxygen vacancies. It is regarded as constant in this n/p mixed regime because $[V_O^{\cdot\cdot}]$ is practically fixed by the effective acceptors $[A']$ at a given temperature.

The total electrical conductivity (σ) may then be represented as

$$\sigma=\sigma_n+\sigma_p+\sigma_{ion}=\sigma_{el,m}\cosh\left[\frac{1}{4}\ln\left(\frac{P_{O_2}}{P_{O_2}^*}\right)\right]+\sigma_{ion}. \qquad (18)$$

C. Chemical diffusivity

When oxide ions and electrons are mobile in BaTiO$_3$, the chemical diffusivity is given in accordance with Wagner as[2]

$$\tilde{D}=-\frac{D_{V_O}t_{el}}{2}\left(\frac{\partial\ln[V_O^{\cdot\cdot}]}{\partial\ln P_{O_2}}\right)^{-1} \qquad (19)$$

or, due to Eq. (17),

$$\tilde{D}=-\frac{kT\sigma_{ion}t_{el}}{8e^2}\left(\frac{\partial[V_O^{\cdot\cdot}]}{\partial\ln P_{O_2}}\right)^{-1}, \qquad (19a)$$

where $t_{el}(=\sigma_{el}/\sigma)$ denotes the electronic transference number. We call the factor within the parentheses a thermodynamic factor. In order to evaluate the chemical diffusivity, one has first to identify t_{el} and the thermodynamic factor in each defect regime.

(i) In the regime $(e', V_O^{\cdot\cdot})$, Eq. (8) yields the thermodynamic factor as

$$\frac{\partial\ln[V_O^{\cdot\cdot}]}{\partial\ln P_{O_2}}=-\frac{1}{6} \qquad (20)$$

and $t_{el}\approx1$ due to Eq. (13). Equation (19) thus takes a familiar form

$$\tilde{D}\approx3D_{V_O}. \qquad (21)$$

(ii) In the regime $(A', V_O^{\cdot\cdot})$, by substituting Eqs. (10) and (11) into Eq. (7), one obtains

$$[V_O^{\cdot\cdot}]=\frac{[A']}{2}+\frac{1}{2}(n-p)=\frac{[A']}{2}-\sqrt{K_i}\sinh\left(\frac{1}{4}\ln\frac{P_{O_2}}{P_{O_2}^0}\right). \qquad (22)$$

Thus the thermodynamic factor takes the form

TABLE I. Parameters, $\sigma_{el,m}$, σ_{ion} and $P_{O_2}^*$, as evaluated from the isotherms of total electrical conductivity.[1]

$T/°C$	$\log_{10}(\sigma_{el,m}/\Omega^{-1}cm^{-1})$	$\log_{10}(\sigma_{ion}/\Omega^{-1}cm^{-1})$	$\log_{10}(P_{O_2}^*/atm)$
800	$-(4.401\pm0.008)$	$-(4.463\pm0.089)$	$-(8.174\pm0.020)$
900	$-(3.756\pm0.008)$	$-(4.155\pm0.065)$	$-(6.400\pm0.020)$
1000	$-(3.191\pm0.010)$	$-(3.681\pm0.083)$	$-(4.772\pm0.025)$
1100	$-(2.740\pm0.015)$	$-(3.272\pm0.100)$	$-(3.447\pm0.041)$

$$\left(\frac{\partial \ln[V_O^{\cdot\cdot}]}{\partial \ln P_{O_2}}\right)^{-1} \approx -\frac{2[A']}{\sqrt{K_i}\cosh\left(\frac{1}{4}\ln\frac{P_{O_2}}{P_{O_2}^0}\right)}. \quad (23)$$

Even if $[V_O^{\cdot\cdot}]$ is practically fixed by acceptor impurities or $[V_O^{\cdot\cdot}]\approx[A']/2$ in this P_{O_2} region, its P_{O_2} dependence is given as that of the difference between the minority carrier concentrations, $n-p$.

Accordingly, due to Eq. (19) or (19a),

$$\tilde{D} = \frac{\tilde{D}^0 t_{el}}{\cosh\left(\frac{1}{4}\ln\frac{P_{O_2}}{P_{O_2}^0}\right)}, \quad (24)$$

where

$$\tilde{D}^0 = \frac{kT\sigma_{ion}}{2e^2\sqrt{K_i}}. \quad (25)$$

III. RESULTS

A. Electronic transference number

The equilibrium total conductivity of undoped BaTiO$_3$ has been repeatedly reproduced as shown in Fig. 2: it varies as $\sigma\propto P_{O_2}^{+1/4}, P_{O_2}^{-1/4}, P_{O_2}^{-1/6}$ as P_{O_2} decreases from 1 atm at the temperatures of interest, which is in accordance with the defect structure in Fig. 4. The conductivity data around the minimum at each temperature that obviously belong to the defect regime $(A',V_O^{\cdot\cdot})$ have earlier been fitted to Eq. (18) as depicted by the solid lines in Fig. 2 and the results, $\sigma_{el,m}$, $P_{O_2}^*$ and σ_{ion}, reported elsewhere.[1] Nevertheless, the latter are reproduced in Table I for immediate reference.

By using the values for σ_{ion} in Table I, one can readily calculate the electronic transference number $(t_{el}\equiv 1 -\sigma_{ion}/\sigma)$ in the regime of $(A',V_O^{\cdot\cdot})$. Outside this regime, obviously $t_{el}\approx 1$; see Eq. (13). The result, t_{el} vs $\log_{10}P_{O_2}$ is as shown in Fig. 5, where the solid lines are the best fitted [see Eq. (18)]. These best-fitted values will be employed later on. As is seen, the electronic transference number at the minimum conductivity decreases (i.e., $t_{el}=0.8–0.55$ at 1100–800 °C) with decreasing temperature. It is noted, however, that t_{el} at 800 °C appears to be somewhat too small compared to what would be expected from the trend at the higher temperatures.
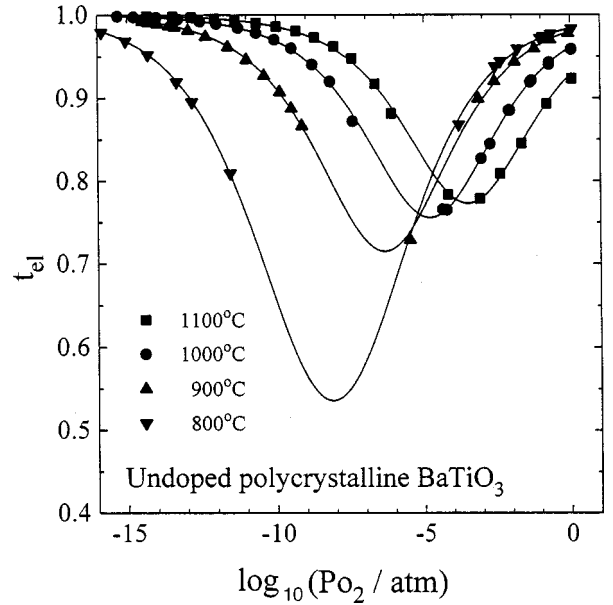
FIG. 5. Electronic transference number against oxygen partial pressure at different temperatures. The solid lines are the best fitted.

B. Chemical diffusivity

Substituting the values for t_{el} in Fig. 5 into Eq. (24), one can evaluate the chemical diffusivity in the n-to-p transition regime or $(A',V_O^{\cdot\cdot})$. In order first to see the variation of $\tilde{D}$ vs $\log P_{O_2}$ schematically and the effect of the mobility ratio $b(=\mu_n/\mu_p)$, the normalized diffusivity $\tilde{D}/\tilde{D}^0$ is plotted for the cases of (a) $b>1$ (or $P_{O_2}^*>P_{O_2}^0$), (b) $b=1$ (or $P_{O_2}^* =P_{O_2}^0$), and (c) $b<1$ (or $P_{O_2}^*<P_{O_2}^0$), respectively, in Fig. 6. It is clearly seen that the chemical diffusivity varies convex upwardly for the given t_{el} in Fig. 5, and its maximum falls to the left of $P_{O_2}^0$ when $P_{O_2}^0<P_{O_2}^*$ and to the right of $P_{O_2}^0$ when $P_{O_2}^*<P_{O_2}^0$. When $b=1$ in particular, $P_{O_2}^*=P_{O_2}^0$ and the minimum of σ_{el} or t_{el} and the maximum of $\tilde{D}$ concur exactly at the (electronic) stoichiometric composition where $n\equiv p$ and $[V_O^{\cdot\cdot}]\equiv[A']/2$. It is pointed out that when $b\neq 1$, a chemical diffusivity isotherm becomes asymmetric about its maximum and can be even distorted locally if the minimum value for t_{el} at $P_{O_2}^*$ is much smaller than the present one.

Upon comparison with the variation of the conductivity isotherms in Fig. 2 and the defect structure in Fig. 4, the diffusivity data in the regions of $\log_{10}(P_{O_2}/atm)<-13$, -11, and -10 at 900, 1000, and 1100 °C, respectively, in Fig. 1 may be regarded as belonging to a transition towards the defect regime of $(e',V_O^{\cdot\cdot})$. They can, thus be fitted to neither Eq. (21) nor Eq. (24). In addition, the two data in $\log(P_{O_2}/atm)>-1$ at 800 °C in particular appear far off the expected from the major trend of variation. It may be attributed to the trapping effect by acceptor-type disorders, as suggested by Bieger et al.[10] and Claus et al.[11] for acceptor-doped SrTiO$_3$ or to the majority type of disorder already being in transition to another regime, say, $(h^{\cdot},A')$ [i.e., no longer in the regime of $(A',V_O^{\cdot\cdot})$]. Those data are thus precluded, and the rest of the data that obviously belong to the n/p mixed regime $(A',V_O^{\cdot\cdot})$ are the best fitted to Eq. (23).
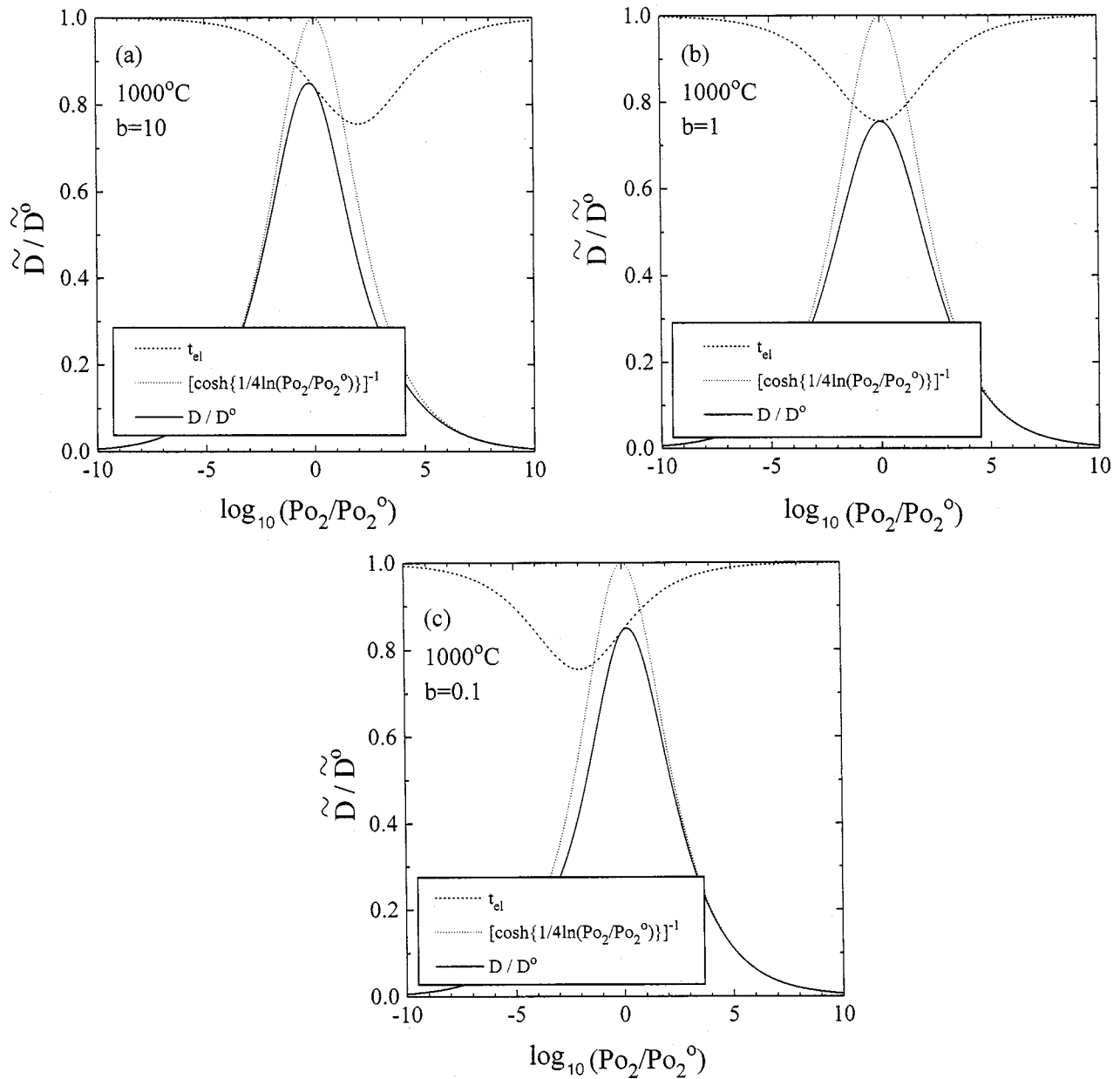
FIG. 6. Normalized chemical diffusivity ($\tilde{D}/\tilde{D}^0$) against oxygen partial pressure at 1000 °C for the cases of (a) $b>1$ (or $P^*_{O_2}>P^0_{O_2}$), (b) $b=1$ (or $P^*_{O_2}=P^0_{O_2}$), and (c) $b<1$ (or $P^*_{O_2}<P^0_{O_2}$), respectively. The dashed and dotted lines are electronic transference number and a P_{O_2}-dependent part of thermodynamic factor, respectively.

The results are as depicted by the solid lines in Fig. 1. The fitting parameters, $\tilde{D}^0$ and $P^0_{O_2}$ are listed in Table II and plotted against reciprocal temperature in Fig. 7 and 8, respectively. In the latter, the values for $P^*_{O_2}$ such that $\sigma_n = \sigma_p$ are

TABLE II. Parameters $\tilde{D}^0$ and $P^0_{O_2}$, as evaluated from the isotherms of chemical diffusivity.

T/°C	$\log_{10}(\tilde{D}^0/\mathrm{cm}^2\,\mathrm{sec}^{-1})$	$\log_{10}(P^0_{O_2}/\mathrm{atm})$
800	$-(2.590 \pm 0.038)$	$-(9.269 \pm 0.151)$
900	$-(2.446 \pm 0.019)$	$-(6.934 \pm 0.080)$
1000	$-(2.364 \pm 0.016)$	$-(5.140 \pm 0.072)$
1100	$-(2.484 \pm 0.015)$	$-(3.725 \pm 0.066)$
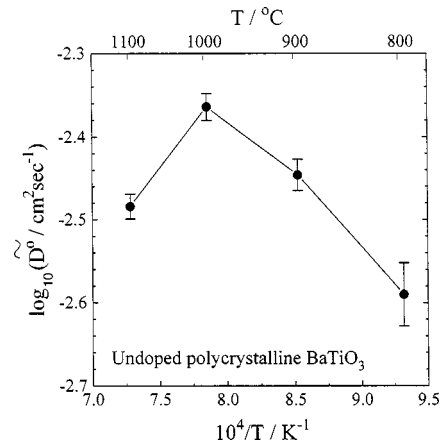
FIG. 7. Evaluated values of $\tilde{D}^0$ at different temperatures.
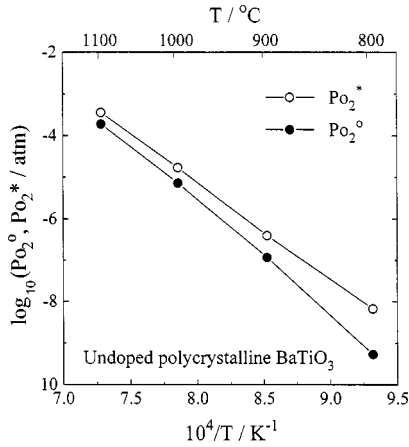
FIG. 8. $\log_{10} P_{O_2}^*$ and $P_{O_2}^0$ vs reciprocal temperature. $P_{O_2}^*$ and $P_{O_2}^0$ are the oxygen partial pressures corresponding to $\sigma_n = \sigma_p$ and $n = p$, respectively.

also plotted for comparison. It is noted that $P_{O_2}^* > P_{O_2}^0$ at all temperatures of examination indicating $b > 1$ upon comparison with Fig. 6.

IV. DISCUSSION

One can recognize that the classic theory, Eq. (19) or Eq. (24), describes quite satisfactorily the measured $\tilde{D}$ in the n-to-p transition region of P_{O_2}. Referring to Fig. 6, the variation of the chemical diffusivity with P_{O_2} is clearly attributed to that of the thermodynamic factor, Eq. (23): A maximum of chemical diffusivity stems from the fact that the thermodynamic factor becomes maximum at the stoichiometric composition where $n \equiv p$. Becker et al.[12] have first reported on the system of α-Ag$_2$S that its chemical diffusivity becomes maximum at the stoichiometric composition and attributed it to the thermodynamic factor becoming maximum there. A similar behavior has later been reported on the system of α-Ag$_2$Te too.[13] Such behavior of $\tilde{D}$ has actually been predicted for the system of BaTiO$_3$ and SrTiO$_3$ in the light of ambipolar diffusion theory,[14] but has never been observed experimentally. The present result is the first observation in oxides in general.

The parameters $\tilde{D}^0$ and $P_{O_2}^0$ in Table II, which have been evaluated from $\tilde{D}$, now enable one to develop further insights into the defect structure of undoped BaTiO$_3$. For this purpose, we need beforehand to have a close look at the ionic conductivity evaluated from Fig. 2.

A. Ionic conductivity

The ionic conductivity values in Table I are plotted against reciprocal temperature in Fig. 9. It is observed that the value at 800 °C is appreciably off the main trend of variation. Rejecting this particular datum, the ionic conductivity may be best estimated as

$$\sigma_{ion} T / \Omega^{-1} \, cm^{-1} \, K = (2.78 \pm 0.16) \times 10^5$$

$$\times \exp\left(-\frac{1.52 \pm 0.01 \, eV}{kT}\right). \quad (26)$$
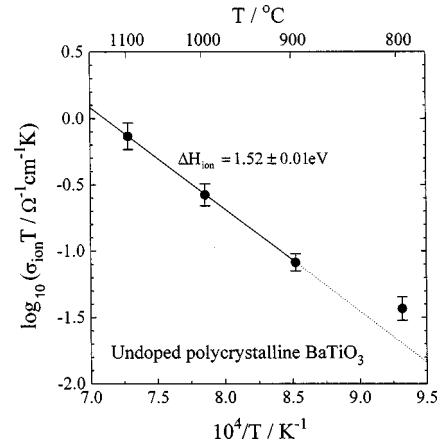
FIG. 9. $\log_{10} \sigma_{ion} T$ vs reciprocal temperature. The solid line is the best fitted with the datum at 800 °C rejected.

The activation energy for ionic conduction, ΔH_{ion}, has been reported as 1.1 eV for undoped BaTiO$_3$.[9,15] The present value of 1.52 eV is somewhat higher; however, the magnitude of the ionic conductivity itself is comparable to that reported[9,15] in the temperature range of interest.

B. Electronic excitation equilibrium constant

Equation (25) is rewritten as

$$K_i = \left(\frac{\sigma_{ion} kT}{2e^2 \tilde{D}^0}\right)^2. \quad (25')$$

By substituting the numerical values for σ_{ion} (Table I) and $\tilde{D}^0$ (Table II), one can evaluate the equilibrium constant K_i for intrinsic electronic excitation reaction, Eq. (4). The result is shown in Fig. 10. It is again seen that the value at 800 °C is higher than the expected from the main trend of variation at the higher temperatures (due to the higher value of σ_{ion} at 800 °C). Rejecting this specific datum at 800 °C, K_i is best estimated as
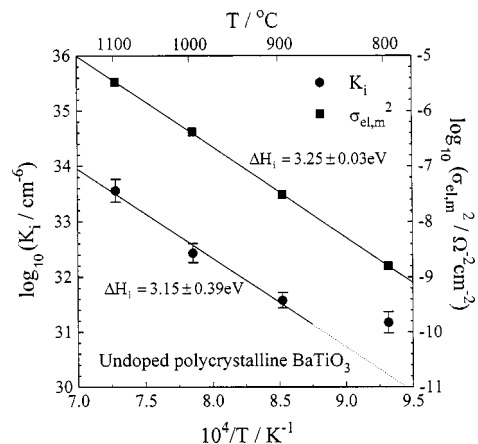
FIG. 10. $\log_{10} K_i$ and $\log_{10} \sigma_{el,m}^2$ vs reciprocal temperature. The solid lines are the best fitted with the datum rejected at 800 °C for K_i.

TABLE III. Comparison of K_i values reported on undoped BaTiO$_3$.

Author(s)	K_i/cm^{-6}	Measurement	Ref.
Song and Yoo	$1.06 \times 10^{45} \exp\left(-\dfrac{3.15\,\text{eV}}{kT}\right)$	Conductivity Chemical diffusivity	This work
Kim et al.	$6.80 \times 10^{44} \exp\left(-\dfrac{2.90\,\text{eV}}{kT}\right)$	Conductivity Thermoelectric Power	3
Seuter	$3.96 \times 10^{46} \exp\left(-\dfrac{3.15\,\text{eV}}{kT}\right)$	Conductivity Thermoelectric Power	16
Nowotny and Rekas	$8.55 \times 10^{44} \exp\left(-\dfrac{2.91\,\text{eV}}{kT}\right)$	Conductivity Thermoelectric Power	17

$$K_i/\text{cm}^{-6} = (1.06^{+36.8}_{-1.03}) \times 10^{45} \exp\left(-\frac{3.15 \pm 0.39\,\text{eV}}{kT}\right) \tag{27}$$

in the temperature range $900 \leq T/°\text{C} \leq 1100$. The band gap is often evaluated from the temperature dependence of the electronic minimum conductivity due to Eq. (15) or

$$K_i = \frac{\sigma^2_{\text{el},m}}{4e^2 \mu_n \mu_p}, \tag{15'}$$

disregarding the temperature dependence of the mobilities μ_n and μ_p. For the present system, the values for $\sigma_{\text{el},m}$ in Table I yield a band gap of 3.25 ± 0.03 eV as shown in Fig. 10, which is quite comparable to the present value, 3.15 ± 0.39 eV. It implies that μ_n and μ_p are very insensitive to temperature in this temperature range.

Up to now only a limited number of data of K_i have been reported for undoped BaTiO$_3$. We compare the present result, Eq. (27), with these reported in Table III. One can recognize that the present one is in general agreement with the reported. This fact strongly supports the validity of the present analysis of chemical diffusivity in terms of Wagner's chemical diffusion theory.[2]

In the conventional evaluation of K_i of BaTiO$_3$, one has had to make assumptions, e.g., on electronic mobilities, density of states, and others.[3,16,17] It is here emphasized that the present K_i has been evaluated only from the experimental data $\tilde{D}^0$ and σ_{ion} without recourse to any assumption at all.

C. Mobilities of electrons and holes

By combining Eqs. (12) and (16), one obtains the mobility ratio b as

TABLE IV. Numerical values for mobilities of electrons and holes.

$T/°\text{C}$	$\mu_n/\text{cm}^2\,\text{V}^{-1}\,\text{sec}^{-1}$	$\mu_p/\text{cm}^2\,\text{V}^{-1}\,\text{sec}^{-1}$
800	0.060 ± 0.019	0.017 ± 0.005
900	0.121 ± 0.025	0.065 ± 0.013
1000	0.151 ± 0.036	0.099 ± 0.024
1100	0.110 ± 0.031	0.080 ± 0.023

$$b = \frac{\mu_n}{\mu_p} = \sqrt{\frac{P^*_{\text{O}_2}}{P^0_{\text{O}_2}}} \tag{28}$$

and, by combining Eqs. (15) and (25), the product of the mobilities:

$$\mu_n \mu_p = \left(\frac{e\,\sigma_{\text{el},m}\tilde{D}^0}{\sigma_{\text{ion}}kT}\right)^2. \tag{29}$$

Only with use of the experimental parameters given in Tables I and II, can one thus determine the two mobilities separately. The results are listed in Table IV and plotted in Fig. 11. The separate determination of the mobilities has been made without using any assumption at all.

In the entire range of temperature of examination, the mobility of electrons is always higher than that of holes or $1.38 \leq b \leq 3.53$. Amazingly, this range of b is in excellent agreement with the expectation $1 < b < 3$ in the literature.[9,15] As temperature increases from 800 °C, both mobilities first increase: however, considering their error bounds, one may regard them as practically independent of temperature above 900 °C. In this temperature range, the average values are $\mu_n = 0.13 \pm 0.02$ cm^2 V^{-1} sec^{-1} and $\mu_p = 0.081 \pm 0.017$ cm^2 V^{-1} sec^{-1}. This is why the activation energy of $\sigma^2_{\text{el},m}$ has turned out to be essentially the same as the true band gap as shown in Fig. 10. It further supports the truthfulness of the
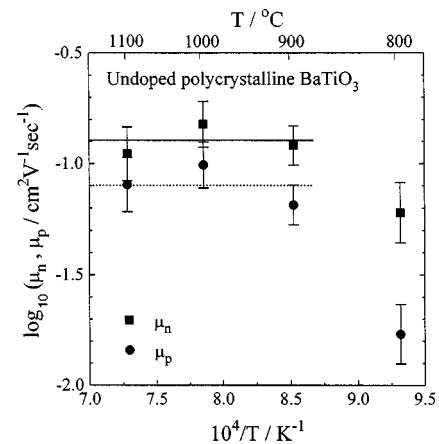
FIG. 11. $\log_{10}\mu_n$ and $\log_{10}\mu_p$ vs reciprocal temperature. The solid and dashed lines denote the average values of μ_n and μ_p, respectively, at temperatures, $900 \leq T/°\text{C} \leq 1100$.

literature values for the band gap of undoped $BaTiO_3$, which were evaluated from the electronic minimum conductivity via Eq. (15).

It is again of interest to compare the present values for the mobilities with the literature values for undoped $BaTiO_3$: $\mu_n = 0.16\,cm^2\,V^{-1}\,sec^{-1}$ (by combining the electrical conductivity and thermopower) in the temperature range of $900 \leq T/^\circ C \leq 1200$,[3] $= 0.2\,cm^2\,V^{-1}\,sec^{-1}$ (in the same manner) at 1000 K;[16] $\mu_p = 0.05\,cm^2\,V^{-1}\,sec^{-1}$ (in the same manner) in the temperature range of $900 \leq T/^\circ C \leq 1200$,[3] $= 0.2\,cm^2\,V^{-1}\,sec^{-1}$ (by Hall measurement) at 700 K.[16]

V. CONCLUSION

The chemical diffusivity of ''undoped'' $BaTiO_{3-\delta}$ as a measure of oxygen nonstoichiomery (δ) reequilibration kinetics is quite well explained by Wagner's classic theory of chemical diffusion or ambipolar diffusion of oxide anions and electrons. The isothermal diffusivity exhibits a maximum approximately at the stoichiometric composition ($\delta = 0$), which originates from the fact that the thermodynamic factor becomes maximum at $\delta = 0$. Combination of the electrical conductivity and chemical diffusivity has enabled one to evaluate, without using any additional assumption at all, the intrinsic electronic excitation equilibrium constant K_i ($= np$) as

$$K_i/cm^{-6} = (1.06^{+36.8}_{-1.03}) \times 10^{45} \exp\left(-\frac{3.15 \pm 0.39\,eV}{kT}\right)$$

and the mobilities of electrons and holes in average as

$$\mu_n = 0.13 \pm 0.02\,cm^2\,V^{-1}\,sec^{-1},$$

$$\mu_p = 0.081 \pm 0.017\,cm^2\,V^{-1}\,sec^{-1}$$

in the temperature range of $900 \leq T/^\circ C \leq 1100$. These results are in fair agreement with those reported.

*Author to whom correspondence should be addressed. FAX: +82-2-884-1413. Electronic address: hiyoo@plaza.snu.ac.kr

[1] C.-R. Song and H.-I. Yoo, Solid State Ionics **120**, 141 (1999).

[2] C. Wagner, Z. Phys. Chem. Abt. B **21**, 25 (1933).

[3] J.-Y. Kim, C.-R. Song, and H.-I. Yoo, J. Electroceram. **1**, 27 (1997).

[4] J. Nowotny and M. Rekas, Solid State Ionics **49**, 135 (1991).

[5] G. V. Lewis and C. R. A. Catlow, Radiat. Eff. **73**, 307 (1983).

[6] S. Shirasaki, H. Yamamura, H. Haneda, K. Kakwgawa, and J. Moori, J. Chem. Phys. **73**, 4640 (1980).

[7] A. Gaecia-Verduch and R. Linder, Ark. Kemi **5**, 313 (1953), quoted in K.-I. Kawamura, A. Saiki, T. Maruyama, and K. Nagata, J. Electrochem. Soc. **142**, 3073 (1995).

[8] J. H. Becker and H. P. R. Frederikse, J. Appl. Phys. **33**, 447 (1962).

[9] N.-H. Chan, R. K. Sharma, and D. M. Smyth, J. Am. Ceram. Soc. **65**, 167 (1982).

[10] T. Bieger, J. Maier, and R. Waser, Sens. Actuators B **7**, 763 (1992).

[11] J. Claus, I. Denk, M. Leonhardt, and J. Maier, Ber. Bunsenges. Phys. Chem. **101**, 1386 (1997).

[12] K. D. Becker, H. Schmalzried, and V. von Wurmb, Solid State Ionics **11**, 213 (1983).

[13] W. Sitte, Solid State Ionics **94**, 85 (1997).

[14] A. Müller and K. H. Härdtl, Appl. Phys. A: Solids Surf. **49**, 75 (1989).

[15] N.-H. Chan, R. K. Sharma, and D. M. Smyth, J. Am. Ceram. Soc. **64**, 556 (1981).

[16] A. M. J. H. Seuter, Philips Res. Rep. Suppl. Int. **3**, 1 (1974).

[17] J. Nowotny and M. Rekas, Ceram. Int. **20**, 225 (1994).